ChemComm

COMMUNICATION

View Article Online
View Journal | View Issue

Cite this: *Chem. Commun.*, 2015, **51**, 16778

Received 31st July 2015,
Accepted 28th September 2015

DOI: 10.1039/c5cc06433c

www.rsc.org/chemcomm

On-surface derivatisation of aromatic molecules on graphene: the importance of packing density†

Sinéad Winters,[ab] Nina C. Berner,[ab] Rohit Mishra,[c] Kim C. Dümbgen,[ab] Claudia Backes,[bc] Martin Hegner,[c] Andreas Hirsch[d] and Georg S. Duesberg*[ab]

An efficient, high-throughput method for the formation of densely packed molecular films on graphene is reported. The films exhibit high stability and remain intact during a subsequent derivatisation reaction, offering a versatile route for the non-covalent functionalisation of graphene.

Graphene has attracted a very high level of interest for gas and bio-molecular sensing applications.[1–4] However, the pristine graphene surface is chemically inert and therefore requires further functionalisation to enable sensor selectivity.[5] Non-covalent functionalisation is an attractive strategy to introduce functional groups on the surface since it does not adversely affect the electronic properties of the graphene sheet.[5–7]

Polycyclic aromatic compounds are generally used to non-covalently bind to graphene *via* π–π stacking.[5] Among them, pyrene-derivatives are the most popular compounds used to introduce functional groups to the graphene surface.[8–10] However, Mann *et al.* revealed that molecules consisting of a single pyrene unit were unstable in organic solution, which prompted the design of compounds consisting of three pyrene ''feet'' in order to form stable films.[11] Further work by the same group revealed that tripod stability increased with the number of aromatic rings contained by the tripod anchor.[12] An alternative method to ensure stability of pyrene on graphene was implemented by Singh *et al.*, who demonstrated electropolymerized pyrene films on graphene for a graphene-based SPR sensor.[13]

Perylene bisimide derivatives with carboxylic acid end-groups have previously shown great potential for the solubilisation of carbon nanotubes (CNTs) and graphene flakes in aqueous solutions.[14]

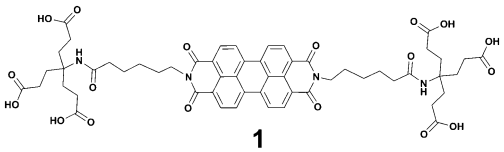

1

Fig. 1 Chemical structure of **1**.

Their core unit is significantly larger than that of pyrene and therefore potentially offers stronger π–π interactions, *i.e.* higher stability. In addition, charge transfer between the perylene and CNTs increases the adsorption of the molecules onto the surface.[15] Due to their previously demonstrated excellent adsorption behaviour, their water solubility for ease of handling and the versatility of carboxylic acid groups for bio-conjugation reactions, we employ a perylene bisimide derivative **1**, (shown in Fig. 1), as the functionalisation agent for CVD-grown graphene in this study.

We have previously shown that wet chemically deposited **1** adsorbs as a monolayer with its aromatic core perpendicular to the graphene surface and that the packing density of the **1** films on CVD graphene is dependent upon the cleanliness of the graphene.[16] More specifically, we found that graphene with polymer residues from the transfer process produces a lower packing density molecular layer than that of graphene that has been annealed to remove these residues, similar to what has been described by other groups.[17,18] In this communication, we demonstrate the ability to functionalise as-grown pristine graphene on Cu foil before polymer transfer to achieve high packing of **1**, avoiding time consuming cleaning procedures. In addition, we show that the molecular layer is very stable which makes it possible to transfer the functionalised graphene to arbitrary substrates in a process we have termed functional layer transfer (FLaT). We are also able to subsequently derivatise the perylene's carboxylic acid groups, which provides a basis for versatile control over the graphene surface chemistry. This has significant implications for the integration of non-covalently functionalised graphene into sensing applications, as often aromatic

[a] *CRANN and School of Chemistry, Trinity College, Dublin, Ireland*
[b] *Advanced Materials and BioEngineering Research (AMBER) Centre, Trinity College, Dublin, Ireland. E-mail: duesberg@tcd.ie*
[c] *CRANN and School of Physics, Trinity College, Dublin, Ireland*
[d] *Institute of Organic Chemistry II, University of Erlangen-Nürnberg, Henkestr. 42, 91054 Erlangen, Germany*

† Electronic supplementary information (ESI) available: Information on graphene quality and transfer. Additional experimental details, AFM images, XPS spectra and Raman map of low density sample pre-derivatisation. See DOI: 10.1039/c5cc06433c

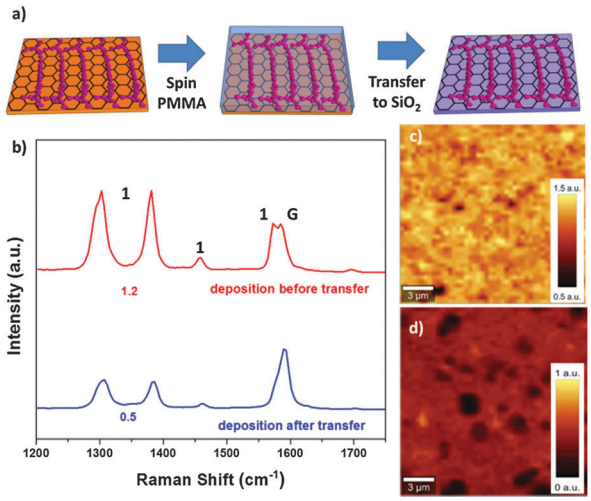

Fig. 2 (a) Schematic of transfer process where molecules are deposited on graphene prior to polymer assisted-transfer. (b) Raman spectra of **1** deposited on graphene *via* modified transfer process (red) and deposited on transferred graphene (blue). The peaks corresponding to **1** and the graphene G band are indicated. (c) Raman map of **1** : G peak ratio for HPD sample after transfer. (d) **1** : G intensity ratio for LPD sample.

molecules are further functionalised with biomolecules in order to produce a selective biosensing surface.[8,19] Stability of the anchor molecules during this further functionalisation process is vital for the development of graphene biosensing devices that require exposure to solvent or aqueous solutions.[6]

The FLaT process where the molecules of **1** are deposited directly onto the as-grown pristine graphene surface on Cu foil before transfer is shown schematically in Fig. 2a. After a solution of **1** is dropcast onto the graphene on Cu, a solution of poly(methylmethacrylate) (PMMA) in anisole is spun over the surface and the copper is removed by ammonium persulfate solution. The resulting PMMA-supported film is transferred onto a substrate and allowed to dry. The PMMA layer is subsequently removed by dissolving in acetone. Raman spectroscopy indicates that a densely packed film of **1** on the graphene surface is still intact after the FLaT process as shown in Fig. 2b (red). **1** can be easily identified by its two main Raman peaks at 1282 cm^{-1} and 1302 cm^{-1}.[20] Generally it is not possible to identify a molecular monolayer by Raman spectroscopy, but due to the GERS effect the Raman signal of the perylene adsorbed on graphene is enhanced.[16,21] The ratio between the **1** peaks and the G band acts as indicator of the packing density of the molecule on the graphene.[16] The high **1** : G ratio of 1.2 obtained from transferring graphene functionalised with **1** is very similar to the ratio (1.5, see ESI†) obtained from our previously reported method of depositing a densely packed layer of **1** on annealed and transferred graphene.[16] We attribute the initial high packing density (HPD) formation to the fact that the as-grown graphene is very clean and the molecular film formation is not disrupted by polymer residue or other contamination. Thus, by utilizing this pre-transfer deposition step, the need for annealing of the graphene substrate is removed. For comparison, an example of a film formed on as-transferred graphene (**1** : G ratio of 0.5), indicating a low packing density (LPD) is also depicted in Fig. 2b (blue). To visualise the presence of **1** on graphene, Raman maps of the **1** : G peak intensity ratio were constructed, as seen in Fig. 2c and d. From these maps it can be observed that the molecular layers form very homogeneous films, with the only irregular (lower density) areas corresponding to areas with second layer graphene growth. It is important to note that films of **1** that have undergone the FLaT process are not disrupted by the additional processing steps, as evidenced by the continuous coverage in Fig. 2c.

The reaction of the carboxylic acid groups of **1** with ethylenediamine (EDA) using *O*-(7-azabenzotriazole-1-yl)-*N*,*N*,*N*′,*N*′-tetramethyluronium hexafluorophosphate (HATU), was investigated as proof-of-concept for the versatile chemistry on graphene achieved by FLaT. The reaction of carboxylic acids with amine groups is a very common process in bioconjugation chemistry; therefore it is important to investigate the feasibility of this reaction in order to determine if the molecules of **1** will be useful anchor units for graphene-based biosensing applications. The method described by Mohanty and Berry[22] for coupling of EDA with graphene oxide surfaces was used. After initiating the reaction, we observe significant differences depending on the original packing density of the perylene molecules, as can be seen in the Raman maps presented in Fig. 3. For samples with a LPD the molecules are removed during the coupling process and are only present in small aggregates on the surface (Fig. 3a). The corresponding Raman spectra for both areas in the sample are shown in Fig. 3b. In the case of the ordered HPD films, the molecules are still present in a uniform film after the functionalisation process, as can be observed in the Raman map of the **1** peak (Fig. 3c). By analysing the average Raman spectra before and after EDA-derivatisation (Fig. 3d), it becomes apparent that the packing density of the molecules has decreased after the reaction (from 1.3 to 1.1). This can most likely be attributed to the increase in carbon chain length upon addition of the EDA, which forces the perylene molecules further apart in order

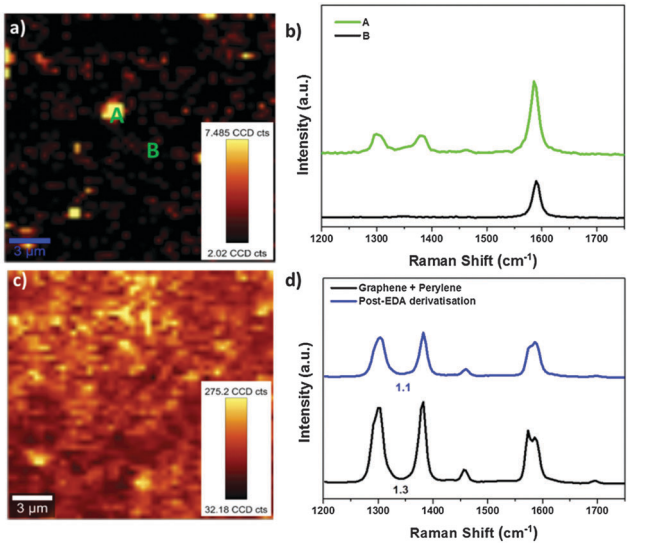

Fig. 3 (a) Raman map of perylene peak intensity after EDA-derivatisation of LPD sample. (b) Corresponding Raman spectra of areas A and B in map. (c) Raman map of **1** peak intensity after EDA derivatisation of HPD sample. (d) Raman spectra of graphene with **1** as-transferred (black) and amine-derivatised **1** on graphene (blue).

to sterically accommodate the longer chains. The disappearance of the anchor molecules during the functionalisation of the LPD samples demonstrates that the formation of ordered films exploiting molecule–molecule interactions is a prerequisite for further derivatisation. This is an important result with regard to understanding the behaviour of molecules during functionalisation on graphene, as it is often assumed that aromatic molecules will adhere strongly to the graphene surface due to π–π stacking, regardless of their adsorption geometry. In this case it can be seen that even with a large aromatic core, **1** can still be removed unless in a densely packed configuration which allows intermolecular forces to stabilise the film.

While the decrease in packing density observed by Raman spectroscopy indicates an increase in the chain length of the end-groups of **1**, X-ray photoelectron spectroscopy (XPS) was employed to confirm the success of the EDA-derivatisation on HPD films. The nitrogen 1s core-level spectrum of **1** as deposited on graphene is shown in Fig. 4 (lower panel). It can be deconvoluted into two contributions, originating from the two different nitrogen environments in the molecule (imide and amide). Their peak areas are roughly equal, with the broader amide component indicating slightly higher disorder in the dendritic tails than in the perylene core. After the reaction with EDA, the deconvolution of the N 1s spectrum shows two additional nitrogen components at the high and low binding energy ends of the overall spectrum as well as an increase of both the amine and amide components' intensities (Fig. 4, middle panel), which is attributed to the expected formation of amide bridges and the appearance of amine terminating groups. The two additional peaks can likely be assigned to the presence of HATU and reaction side-product residues (inset, middle panel), which contain other nitrogen species. The HATU reagent residue is largely removed by briefly annealing the sample at 220 °C as can be seen in the significant decrease of those two additional components in Fig. 4 (upper panel). The amine component still appears to be larger than the amide component after the annealing step, which is surprising since any derivatisation of the –COOH end-groups to amide bridges and amine termini would have equal amounts of amines and amides. In addition, physisorbed EDA would have desorbed at 220 °C. However, the deconvolution and extraction of relative intensities of the components are comparatively challenging in this case due to the high FWHM of the peaks and the high number of different nitrogen containing compounds involved in the reaction. Despite a large error margin, the overall significantly increased intensity of amine and amide components after annealing indicates that the EDA has at least partially successfully coupled with the –COOH groups on the **1** "anchor"-molecule. Due to the perpendicular orientation of the molecules on the graphene,[16] we do not expect full coupling to occur as at least one –COOH group will be obscured by the presence of those above.

In order to further verify the presence of amine end-groups on the graphene surface, the adhesion of bacteria was tested using fluorescence microscopy. *Escherichia coli* (*E. coli*) are gram-negative bacteria, with a negatively charged cell wall,[23] which are attracted to positively charged amine groups due to electrostatic interactions.[22] Fluorescence images of *E. coli* bacteria on bare graphene as well as graphene/**1** before and after the **1** derivatisation are presented in Fig. 5. On bare graphene and graphene with **1** (Fig. 5a and b) only a few bacteria are present, which is attributed to non-specific adsorption as the graphene surface contains no charge to attract the *E. coli*. The graphene/**1** surface is decorated with negative charges due to deprotonated carboxylic acid groups which repel the negatively charged bacteria. In contrast, the amine-modified **1** surface (Fig. 5c) has an order of magnitude higher density of bacteria present on the surface, thus indicating strong interactions between bacteria and the charged surface due to the presence of amine groups on the functionalised graphene. Fig. 5d shows a histogram of the average number of bacteria present on the different surfaces. The bare graphene and graphene with **1** contain 0.9 (±0.5) bacteria × 10^4 cm^{-2} and 2.6 (±0.9) bacteria × 10^4 cm^{-2}, respectively. In contrast, the amine functionalised sample contains 11.7 (±4.8) bacteria × 10^4 cm^{-2}. This ability of the derivatised graphene surface to immobilise bacteria from a solution has potential to be harnessed to detect bacteria using optical, mechanical or electrical sensors.

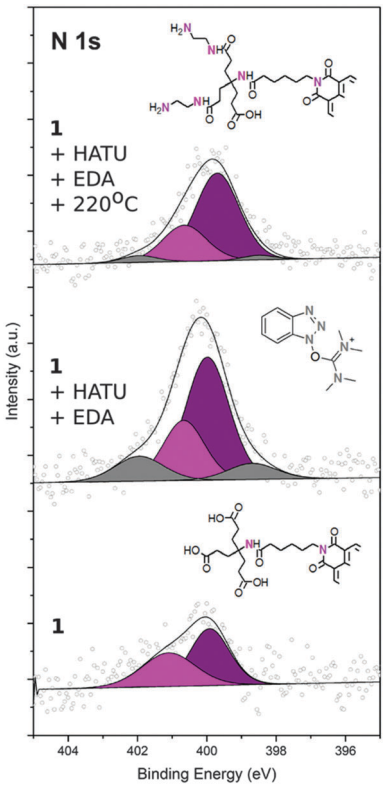

Fig. 4 Evolution of XPS spectra of perylene on graphene. Lower panel: As-transferred **1** on graphene. Inset: Partial structure of **1** with corresponding nitrogen contributions. Middle panel: **1** on graphene after reaction with HATU and EDA. The two new contributions are from HATU residue. Inset: Chemical structure of HATU. Upper panel: After 220 °C anneal of derivatised sample. The HATU contributions have been reduced, but the amine signal is still increased. Inset: Partial structure of **1** after reaction, depicting corresponding nitrogen contributions.

To conclude, we have introduced a method of depositing perylene-based molecules onto pristine CVD graphene, which produces molecular layers with high packing density on the graphene surface. This FLaT technique is scalable and can be

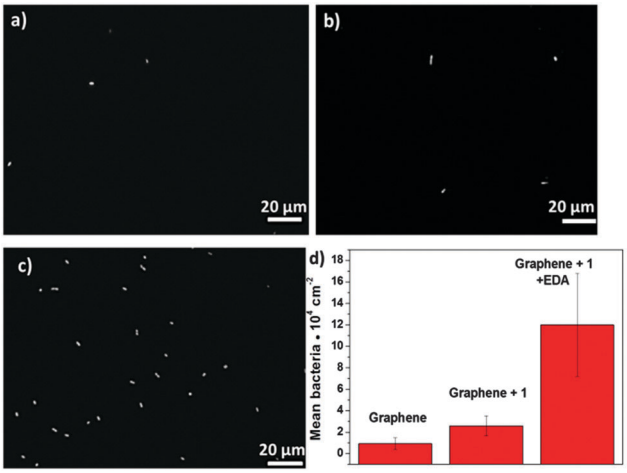

Fig. 5 Fluorescence images of *E. coli* bacteria on (a) graphene (b) graphene functionalised with **1** and (c) **1** on graphene after amine-functionalisation. (d) Histogram indicating the average number of bacteria on each sample.

used to produce large areas of non-covalently functionalised graphene while reducing sample preparation time as it eliminates the need to anneal the graphene in order to remove polymer residue and achieve high density films.

The significantly increased stability of the HPD films has been demonstrated during an on-surface derivatisation process. For LPD **1** films, the molecules are removed during a coupling reaction, while the HPD film remains stable. This observation is vital to the integration of graphene into biosensors as their selectivity hinges upon the ability of the aromatic molecules to anchor selective antibodies to the graphene surface. Therefore the packing density and stability of any potential aromatic anchor must be assessed before use in a biosensor. The proof-of-concept alteration of the functional end-groups of **1** from carboxylic acid to amine has been characterised by Raman spectroscopy and XPS. In addition, fluorescence images demonstrate increased adhesion of *E. coli* bacteria to the amine-functionalised graphene. This opens the path to the integration of these films into graphene-based bacterial and a large variety of other biomolecular sensing devices.

S.W., N.C.B. and G.S.D. acknowledge SFI under grant number PI_10/IN.1/I3030. R.M. and M.H. also thank SFI under PI grant SFI/09IN/1B2623. C.B. is supported by the German research foundation DFG (BA 4856/1-1). A.H. thanks the DFG (SFB 953 Synthetic Carbon Allotropes) for financial support.

References

1 K. R. Ratinac, W. R. Yang, S. P. Ringer and F. Braet, *Environ. Sci. Technol.*, 2010, **44**, 1167–1176.
2 M. D. Angione, R. Pilolli, S. Cotrone, M. Magliulo, A. Mallardi, G. Palazzo, L. Sabbatini, D. Fine, A. Dodabalapur, N. Cioffi and L. Torsi, *Mater. Today*, 2011, **14**, 424–433.
3 Y. Liu, X. Dong and P. Chen, *Chem. Soc. Rev.*, 2012, **41**, 2283–2307.
4 Y. Y. Shao, J. Wang, H. Wu, J. Liu, I. A. Aksay and Y. H. Lin, *Electroanalysis*, 2010, **22**, 1027–1036.
5 V. Georgakilas, M. Otyepka, A. B. Bourlinos, V. Chandra, N. Kim, K. C. Kemp, P. Hobza, R. Zboril and K. S. Kim, *Chem. Rev.*, 2012, **112**, 6156–6214.
6 J. A. Mann and W. R. Dichtel, *J. Phys. Chem. Lett.*, 2013, **4**, 2649–2657.
7 J. H. Yuan and K. M. Liew, *Mater. Chem. Phys.*, 2014, **145**, 313–319.
8 Y. X. Huang, X. C. Dong, Y. X. Liu, L. J. Li and P. Chen, *J. Mater. Chem.*, 2011, **21**, 12358–12362.
9 S. Ghosh, X. H. An, R. Shah, D. Rawat, B. Dave, S. Kar and S. Talapatra, *J. Phys. Chem. C*, 2012, **116**, 20688–20693.
10 X. Dong, D. Fu, W. Fang, Y. Shi, P. Chen and L. J. Li, *Small*, 2009, **5**, 1422–1426.
11 J. A. Mann, J. Rodríguez-López, H. D. Abruña and W. R. Dichtel, *J. Am. Chem. Soc.*, 2011, **133**, 17614.
12 J. A. Mann and W. R. Dichtel, *ACS Nano*, 2013, **7**, 7193–7199.
13 M. Singh, M. Holzinger, M. Tabrizian, S. Winters, N. C. Berner, S. Cosnier and G. S. Duesberg, *J. Am. Chem. Soc.*, 2015, **137**, 2800–2803.
14 C. Backes, F. Hauke and A. Hirsch, *Adv. Mater.*, 2011, **23**, 2588–2601.
15 C. Ehli, C. Oelsner, D. M. Guldi, A. Mateo-Alonso, M. Prato, C. Schmidt, C. Backes, F. Hauke and A. Hirsch, *Nat. Chem.*, 2009, **1**, 243–249.
16 N. C. Berner, S. Winters, C. Backes, C. Yim, K. C. Dümbgen, I. Kaminska, S. Mackowski, A. A. Cafolla, A. Hirsch and G. S. Duesberg, *Nanoscale*, 2015, DOI: 10.1039/C5NR04772B.
17 W. H. Lee, J. Park, S. H. Sim, S. Lim, K. S. Kim, B. H. Hong and K. Cho, *J. Am. Chem. Soc.*, 2011, **133**, 4447–4454.
18 M. Kratzer, B. C. Bayer, P. R. Kidambi, A. Matkovic, R. Gajic, A. Cabrero-Vilatela, R. S. Weatherup, S. Hofmann and C. Teichert, *Appl. Phys. Lett.*, 2015, **106**, 103101.
19 J. A. Mann, T. Alava, H. G. Craighead and W. R. Dichtel, *Angew. Chem., Int. Ed.*, 2013, **52**, 3177–3180.
20 N. V. Kozhemyakina, J. M. Englert, G. Yang, E. Spiecker, C. D. Schmidt, F. Hauke and A. Hirsch, *Adv. Mater.*, 2010, **22**, 5483–5487.
21 X. Ling, L. Xie, Y. Fang, H. Xu, H. Zhang, J. Kong, M. S. Dresselhaus, J. Zhang and Z. Liu, *Nano Lett.*, 2010, **10**, 553–561.
22 N. Mohanty and V. Berry, *Nano Lett.*, 2008, **8**, 4469–4476.
23 T. J. Silhavy, D. Kahne and S. Walker, *Cold Spring Harbor Perspect. Biol.*, 2010, **2**, a000414.